Intermolecular Potential of the O_2-O_2 Dimer. An ab Initio Study and Comparison with Experiment†

Ramón Hernández-Lamoneda*

Centro de Investigaciones Químicas, Universidad Autónoma del Estado de Morelos, 62210 Cuernavaca, Mor., México

Massimiliano Bartolomei

Dipartimento di Chimica, Universitá di Perugia, 06123, Perugia, Italy

Marta I. Hernández and José Campos-Martínez

Instituto de Matemáticas y Física Fundamental, Consejo Superior de Investigaciones Científicas, Serrano 123, 28006 Madrid, Spain

Fabrice Dayou

Laboratoire d'Etude du Rayonnement et de la Matière en Astrophysique, UMR 8112 du CNRS, Observatoire de Paris-Meudon, 5 place Jules Janssen, 92195 Meudon Cedex, France

Received: July 7, 2005

Accurate intermolecular potentials for the lowest three multiplet states of O_2-O_2 dimer have been produced on the basis of ab initio calculations. The quintet potential was taken from previous highly correlated CCSD-(T) calculations. In this work, we perform MRCI calculations, with large basis sets including bond functions, of the singlet and triplet states, which are of multireference character. As expected the size inconsistency and lack of higher order excitations limit the accuracy of the MRCI potentials specifically in describing the long range interactions. We show that the Heisenberg Hamiltonian provides an accurate representation of the exchange interactions in this system and this enables us to combine the accurate CCSD(T) potentials with the MRCI spin-exchange parameter to obtain accurate singlet and triplet potentials. The reliability of these potentials is tested by computing integral cross sections and comparing them with the detailed experimental study of the Perugia group, with excellent results. More interestingly, comparison with the experimentally derived potential shows important discrepancies for some angular orientations including that corresponding with the global minima, indicating the need for further work, both theoretical and experimental, to clarify their origin.

I. Introduction

The study of van der Waals molecules is a topic of general interest in the physical sciences with far reaching implications in other areas such as the life sciences.[1] The weak intermolecular forces that bind these systems determine a rich variety of structural, spectroscopical, and dynamical properties which are the subject of both experimental and theoretical scrutiny using state of the art methodology.[1] One of the reasons that the area has continued to be prolific in recent years is the interplay between experiment and theory, where, for small systems, the level of detail and accuracy of measurements and calculations are evenly matched. Furthermore, each development in either approach pushes the other one in a positive feedback chain.

Among the van der Waals systems which remain a challenge, even for small size systems, are those of open-shell nature. For these systems additional features arise, such as low-lying electronic states, spin−orbit coupling, and nonadiabatic effects, which further complicate their accurate description.[2] Furthermore, from the point of view of calculating a potential energy surface (PES) via ab initio methods, such systems require the use of multiconfigurational wave functions to properly describe the features mentioned above. Unfortunately, these type of methods suffer from size extensivity problems and generally do not include dynamical electron correlation at the high order required for an accurate determination of the weak intermolecular forces. In this regard, we have to mention the two methods which have proved to be the most reliable: the CCSD-(T)[3] coupled cluster method, which includes electron correlation through high orders and is often considered as providing benchmark results, and the symmetry-adapted perturbation theory approach[4] (SAPT), which provides an excellent framework to analyze the components of the interaction energy and thus identify and correct sources of error. Unfortunately both methods rely on the validity of a single reference expansion of the wave function and cannot be generally applied to open-shell species. These points illustrate the need for further progress in developing a new ab initio methodology.

Molecular oxygen dimer O_2-O_2 is a good example of an interesting open-shell species with unique properties. The fact that the monomer has a triplet ground state leads to three possible intermolecular potentials for the dimer with singlet, triplet, and quintet multiplicities, which determine its unique structural, spectroscopical, and dynamical properties, all of

* Corresponding author. E-mail: ramon@servm.fc.uaem.mx.
† Part of the special issue "Jack Simons Festschrift".

10.1021/jp053728g CCC: $30.25
Published on Web 10/25/2005

which have been the subject of many past and recent studies. The nature of its binding was a topic of interest for early theoretical speculations by Lewis[5] and Pauling.[6] Long and Ewing[7] were the first to observe this species at low temperatures using collision-induced spectroscopy. From their study it was clear that the complex was bound by weak intermolecular forces. Goodman and Brus[8] trapped the dimer in a neon matrix and concluded, from high resolution spectra, that the ground state is a singlet with low-lying triplet and quintet electronic states. Their spectra was only consistent with a D_{2h} or D_{2d} symmetry for the complex. More recently it has become clear that the properties of the dimer are of relevance in a variety of phenomena: collisional and radiative processes in the atmosphere,[9] the chemical oxygen iodine laser,[10] and the properties of new condensed phases of oxygen.[11]

The accurate determination of the intermolecular potential and the associated physical properties of the oxygen dimer has proven to be a challenge for both experiment and theory. Although the spectroscopical work mentioned above provided valuable general information on the complex, it could not produce rotationally resolved spectra due to the collision-induced nature of the experiment. From the theoretical point of view, it is worth mentioning the intermolecular potential developed by Bussery and Wormer[12] (BW) constructed from first-order (electrostatic and exchange) contributions at the Hartree−Fock level[13] and the second-order polarization energy is evaluated through a semiempirical procedure proposed by Cambi et al.,[14] circumventing in this way the difficulty inherent to an ab initio determination of the dispersion terms.

The most complete and accurate determination of the oxygen dimer intermolecular potential to date was realized in scattering of both rotationally hot and rotationally cold (with control of the alignment degree) O_2 molecular beams with O_2 target molecules by the Perugia group.[15] By using a spherical harmonic expansion of the potential, they determined the associated radial coefficients fitting relatively few parameters to reproduce the measured integral cross sections, including glory oscillations which are highly sensitive to the well and long-range part of the potential. Comparison with the theoretical BW potential indicated an overall agreement regarding qualitative features such as relative stability with respect to the spin state and angular orientation but significant quantitative differences exist, most notably, the theoretical underestimation of binding energies for the linear and T-shaped geometries. Significant differences arise also for the equilibrium center of mass distances (R_e) for the D_{2h} and D_{2d} angular configurations, with theoretical values being shorter by a few tenths of an angstrom. In this respect it is worth mentioning that a rotationally resolved spectrum of the O_2-O_2 dimer was recently obtained.[16] The spectrum is highly congested but, with the help of bound state calculations on the BW surface, could be analyzed. They confirm the D_{2h} symmetry of the ground state and predict an R_e close to the theoretical estimate.

For the quintet state of O_2-O_2 a single configuration reference provides an acceptable zeroth-order wave function (which is not the case for the other multiplicities) so that it is possible to apply the RCCSD(T) method to obtain an accurate ab initio intermolecular potential. We recently[17] performed such calculations providing the best theoretical quintet potentials to date. Comparison with the Perugia potential showed an excellent agreement (differences of less than 5%) for the binding energies as a function of the angular and radial coordinates for most geometries studied, but a surprising disagreement was observed for the linear configuration: the theoretical value is larger by $\approx$65%. Furthermore, appreciable differences were found for the R_e values of the D_{2h} and D_{2d} angular configurations which coincide with the global minimum for the singlet and quintet states, respectively. The theoretical estimates are shorter by a few tenths of an angstrom in analogy to the singlet case discussed above.

The objective of the present work is to perform high quality ab initio calculations on the singlet and triplet states, which cannot be studied with the RCCSD(T) method, to obtain the most reliable set of theoretical potentials to date. Clearly it is a challenge for multireference ab initio methods to match the excellent agreement with experiment obtained for the quintet state with the RCCSD(T) method.[17] We will show that, by a judicious combination of the ab initio information, we can reproduce most of the detailed features in the cross sections measured by the Perugia group.

II. Methodology

Four geometrical arrangements of the dimer O_2-O_2 have been considered for the present study: linear ($D_{\infty h}$), T-shaped (C_{2v}), rectangular (D_{2h}), and crossed (D_{2d}) structures. We will name them L, T, H, and X, respectively, as is customary for this system. To test basis set saturation, we have selected three progressively larger basis sets. First we use the 5s4p3d2f ANO basis set,[18] which we have employed in previous studies for this system and which is designed to recover a large fraction of the atomic correlation energy. The basis will be denoted by B1 throughout the present study. The importance of including bond functions in order to accurately represent the weak dispersion forces is well established.[19] Therefore, we have added the bond function set [3s3p2d] developed by Tao.[20] In that study, it was shown that with this set excellent results were obtained for the extremely small interaction energy in helium dimer, and they proved that inclusion of the bond functions allows to replace high angular momentum functions centered in the atoms. The latter basis set will be denoted B2. Finally in order to further test the basis saturation, we increased the B1 basis to 6s5p3d2f and added an extra f function for the bond function set to yield [3s3p2d1f], named B3 hereafter. The bond functions are placed in the middle of the complex as is customary.

To treat the near-degeneracies present in this system it is mandatory to use multiconfiguration based methods. In a first step we optimize the orbitals of the given state using the CASSCF method. Subsequently the multiconfiguration wave function so obtained is used as a reference to perform MRCI calculations in order to include dynamical correlation effects. Two active spaces have been used: the first one distributes 16 electrons in 12 active molecular orbitals correlating with the oxygen atomic p shell. For the smallest basis set B1, the lowest symmetry geometries and the singlet state this choice leads to MRCI expansions of roughly 10^8 contracted configurations (10^{11} uncontracted configurations). With such a size, the study of basis set saturation would be extremely demanding, though possible. Since we are only interested in a limited region of configurational space and, in particular, we do not explore the stretching of bonds in the system, it is possible to reduce the active space by looking at the occupation numbers of the natural orbitals resulting from the previously mentioned MRCI wave functions. This allows us to define a smaller active space of 12 electrons in 8 active orbitals, which lead to easily manageable MRCI expansions and the study of basis saturation. The adequacy of this choice will be illustrated in the next section. The two types of calculation will be denoted hereafter MRCI-1 for the smaller active space and MRCI-2 for the larger. One of the main sources of error with the present methodology is the fact that the MRCI

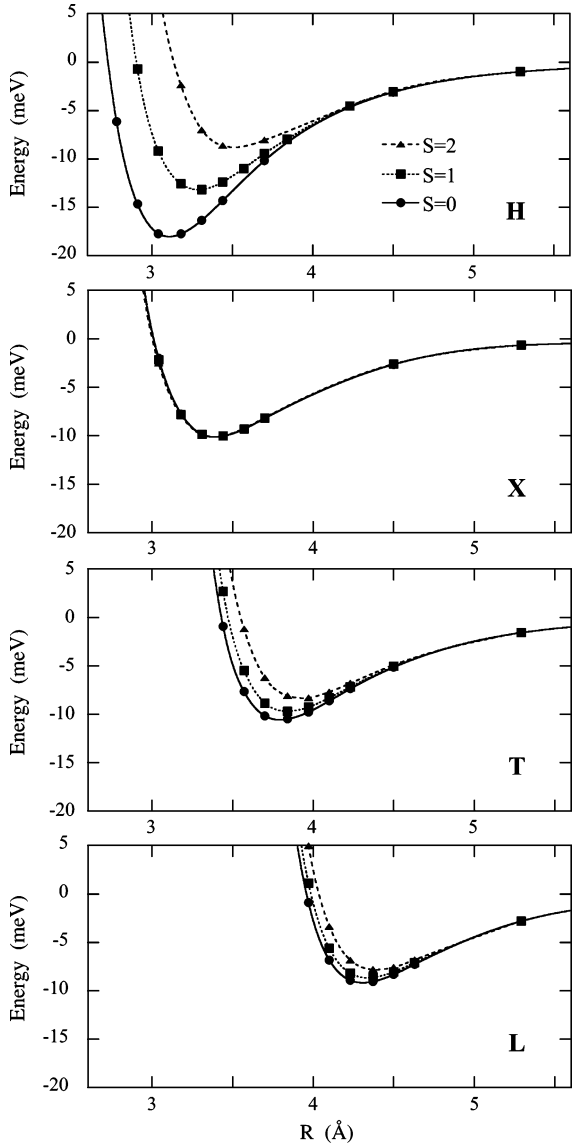

Figure 1. Interaction potentials associated with the first singlet ($S = 0$), triplet ($S = 1$), and quintet ($S = 2$) states of the dimer O_2-O_2 in four selected geometries as obtained from MRCI calculations at the MRCI-1/B3 level of theory.

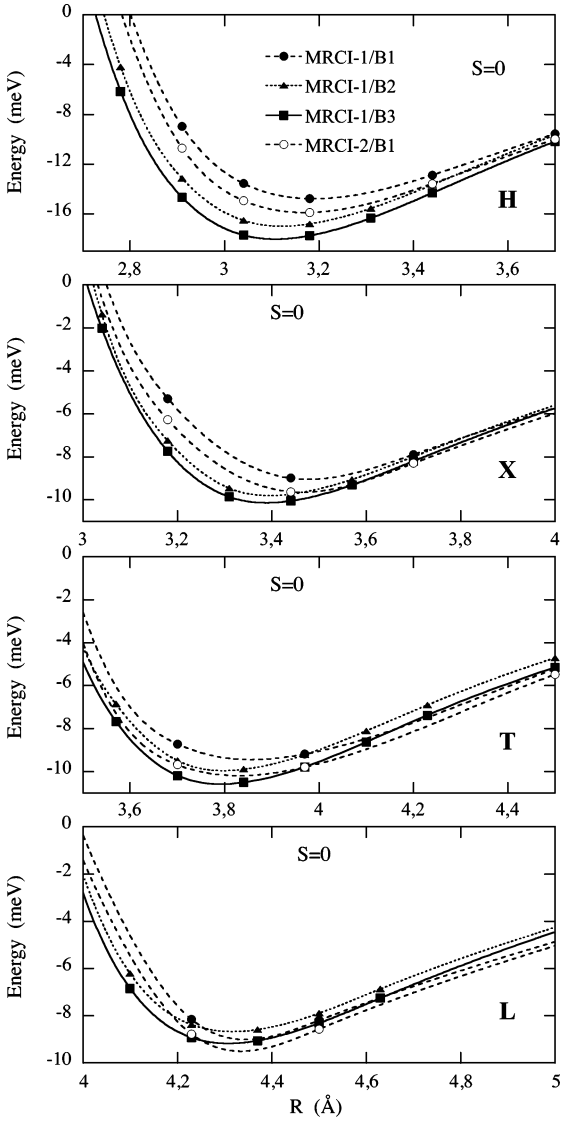

Figure 2. Comparison of interaction potentials associated with the first singlet state ($S = 0$) of the dimer O_2-O_2 in four selected geometries as obtained from MRCI calculations at different levels of theory.

method is not size consistent. To improve our predictions, we thus apply the Davidson's correction.[21,22] Another important source of error comes from basis set superposition, and we apply the counterpoise procedure[23,24] to obtain the final interaction energies.

III. Results and Discussion

A. MRCI Test Calculations. Results of MRCI calculations for the first singlet, triplet, and quintet states of the dimer O_2-O_2 are presented in Figures 1−3 and Table 1. A summary of all the computations using the MRCI-1/B3 level of theory is given in Figure 1. A qualitative agreement with the intermolecular potential of the Perugia group[15] is found. For both, theoretical and experimental potentials, X is the most stable configuration for the quintet state whereas H is the most stable one for singlet and triplet states. Also, the ordering of the binding energies and the equilibrium positions is the same in both sets, for instance, for the singlet state, binding energies decrease and equilibrium positions increase for configurations H, T, X, L and H, X, T, L, respectively. The splitting due to spin−spin interaction is also similar within each angular orientation.

At this point and for reasons that will become apparent soon, we do not attempt to compare in more detail with the Perugia empirical potential, and we turn to a more detailed analysis of the MRCI calculations. In Figure 2, we report the interaction potentials obtained for the singlet state in several different levels of theory, and in Table 1, we summarize the equilibrium properties for all multiplicities and geometries. Focusing on the H geometry, it can be seen that the binding energy increases substantially when adding the first set of bond functions (≈15% from B1 to B2) but shows only a small increase when further increasing the basis set (≈6% from B2 to B3) indicating that we are close to saturation. On the other hand, the equilibrium bond length becomes shorter upon increasing the basis set. A very similar basis set dependence was observed in ref 17 in CCSD(T) calculations for the quintet state using the same three sets of basis functions. We can also compare the relative performance of the two active spaces used with the smallest basis set (MRCI-1/B1 and MRCI-2/B1), and as expected, the larger calculation yields a larger binding energy (≈8%) and only slightly shorter equilibrium bond length, suggesting that the smaller space is already an adequate option. Another test of this choice can be performed by looking at the relative weight of the reference wave function in the total expansion, and here

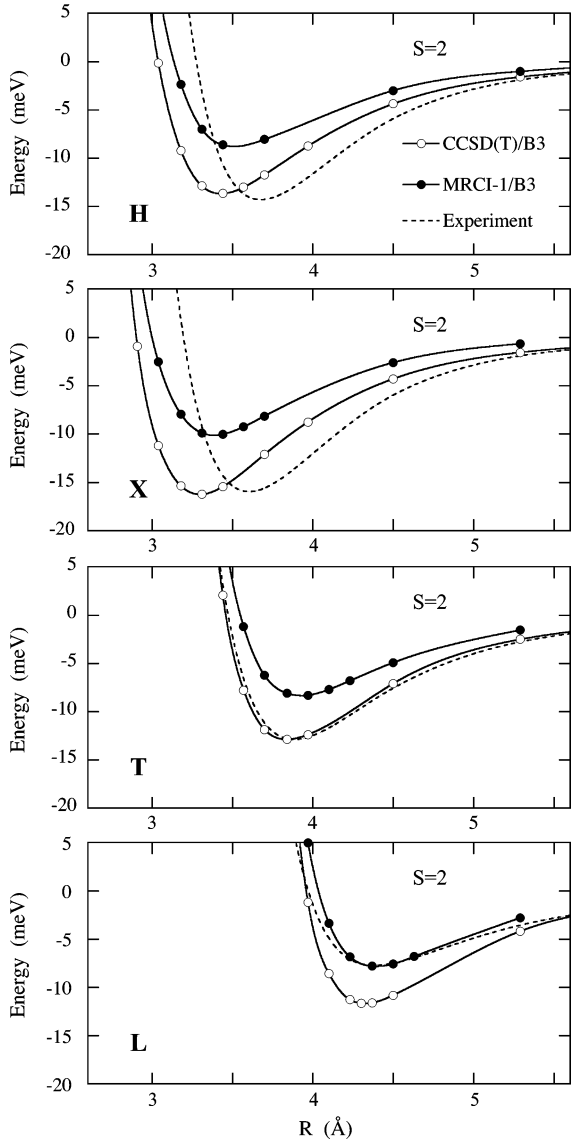

Figure 3. Comparison of interaction potentials associated with the first quintet state ($S = 2$) of the dimer O_2-O_2 in four selected geometries as obtained from ab initio calculations (CCSD(T) and MRCI approaches) and deduced from the molecular beam experiment.[15]

we observe values always above 90%. As a final check on this issue, we performed single point calculations, using the best estimate for the equilibrium geometry, with the largest active space and basis set (MRCI-2/B3) for which the binding energy increased by about 8% relative to the smaller active space (MRCI-1/B3). The same test was performed for the quintet state, yielding an increase of 7% in the binding energy. Considering that the difference in computational costs for the two selected active spaces is nearly 3 orders of magnitude, the adequacy of selecting a smaller active space is evident. For the triplet and quintet state in the H geometry, we have found the same trends regarding basis set and active space dependence (see Table 1). The basis set and active space dependence also is similar for the X and T geometries, although the variation in the binding energies is weaker than that found for the H orientation (see Figure 2 and Table 1). Finally, for the L geometry, we also observe a weaker basis set dependence although we notice that adding bond functions (from B1 to B2) yields a slight decrease in the binding energy. We have also performed single point calculations at the equilibrium geometry of the L configuration in its quintet state using the largest active space and basis set under study (MRCI-2/B3 calculations). As expected the binding energies did not change significantly with respect to the smaller active space (MRCI-1/B3 calculations), around 6%, whereas the CPU time for these calculations scaled up roughly 3 orders of magnitude clearly indicating that the MRCI-1/B3 level of theory is the choice providing the best balance between the computational cost and a adequate description of interaction energies.

TABLE 1: Equilibrium Distances R_e (in Å) and Binding Energies D_e (in meV) for the Singlet, Triplet, and Quintuplet States of the Dimer $(O_2)_2$ in Four Selected Geometries As Obtained from MRCI Calculations at Different Levels of Theory (See Text)

		H		X		T		L	
	calculation	R_e	D_e	R_e	D_e	R_e	D_e	R_e	D_e
singlet	MRCI-1/B1	3.19	14.8	3.48	9.0	3.86	9.4	4.34	9.0
	MRCI-1/B2	3.12	17.0	3.39	9.8	3.80	10.0	4.32	8.7
	MRCI-1/B3	3.11	18.0	3.39	10.1	3.79	10.6	4.31	9.2
	MRCI-2/B1	3.17	15.9	3.46	9.6	3.83	10.2	4.33	9.5
triplet	MRCI-1/B1	3.37	11.1	3.48	9.0	3.91	8.8	4.36	8.6
	MRCI-1/B2	3.31	12.4	3.39	9.8	3.84	9.1	4.34	8.2
	MRCI-1/B3	3.29	13.2	3.39	10.1	3.84	9.7	4.34	8.7
	MRCI-2/B1	3.36	11.8	–	–	–	–	–	–
quintet	MRCI-1/B1	3.56	8.0	3.48	9.0	4.01	7.8	4.36	8.7
	MRCI-1/B2	3.52	8.2	3.39	9.8	3.94	7.8	4.40	7.4
	MRCI-1/B3	3.51	8.8	3.38	10.1	3.93	8.3	4.39	7.8
	MRCI-2/B1	3.55	8.4						
	CCSD(T)/B3[b]	3.43	13.7	3.30	16.2	3.84	12.9	4.33	11.7

[a] For the quintet state, the results of recent CCSD(T) calcualtions[17] are also reported. [b] Values corresponding to the PES of Ref 17.

A further and important test of the MRCI calculations is the comparison with the very accurate CCSD(T) method in the case of the quintet state. In Figure 3, the MRCI-1/B3 interaction potentials associated with this multiplicity are compared to those resulting from the CCSD(T) approach using the same basis set.[17] The Perugia potential is also shown in this figure. Equilibrium properties from CCSD(T)/B3 calculations are given in Table 1. It is readily seen that both theoretical approaches provide rather similar values of the equilibrium bond lengths, but the MRCI approach underestimates the binding energies for all the orientations studied and in a very important proportion. This result clearly indicates that whereas the basis set and active space used are satisfactory given the weaker dependences discussed in the previous paragraph, the MRCI method does not provide the level of correlation needed to quantitatively describe the dispersion forces in the interaction between oxygen molecules. This is the reason we do not find pertinent to compare present MRCI and Perugia potentials at a quantitative level. As an example of how this comparison could lead to misleading conclusions, it can be seen that MRCI and Perugia quintet potentials are in excellent agreement for the L geometry (lowest panel of Figure 3). After the comparison between the MRCI and CCSD(T) methods, clearly indicating the MRCI underestimation of dispersion energies, one must conclude that this agreement with the experimentally based potential is fortuitous.

B. CCSD(T)/MRCI Mixed PES. The theoretical interaction potentials depicted in Figure 3 clearly show the superiority of the coupled cluster approach over the MRCI method to provide accurate binding energies in the case of weakly bonded systems. Nevertheless, until multireference coupled cluster methods become routinely available the method is still limited to cases where the electronic state under study can be well represented by a single configuration wave function. For the dimer O_2-O_2 such a limitation restricts the use of the coupled cluster approach to the first quintet state. On the other hand, the energy splitting

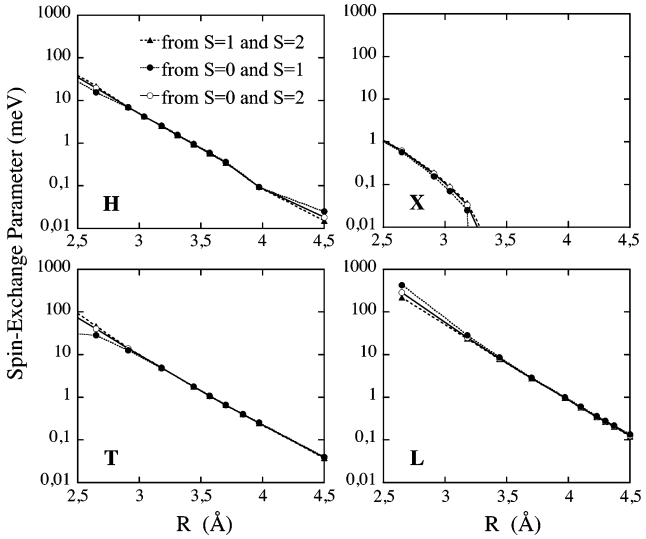

Figure 4. Absolute values of the spin-exchange parameter $|J|$ from MRCI-1/B3 energies as a function of the intermolecular separation in four selected geometries of the dimer O_2-O_2. The values are given by $|J| = (1/2)|V(S = 0) - V(S = 1)|$ (filled circles), $|J| = (1/4)|V(S = 1) - V(S = 2)|$ (filled triangles), and $|J| = (1/6)|V(S = 0) - V(S = 2)|$ (open circles).

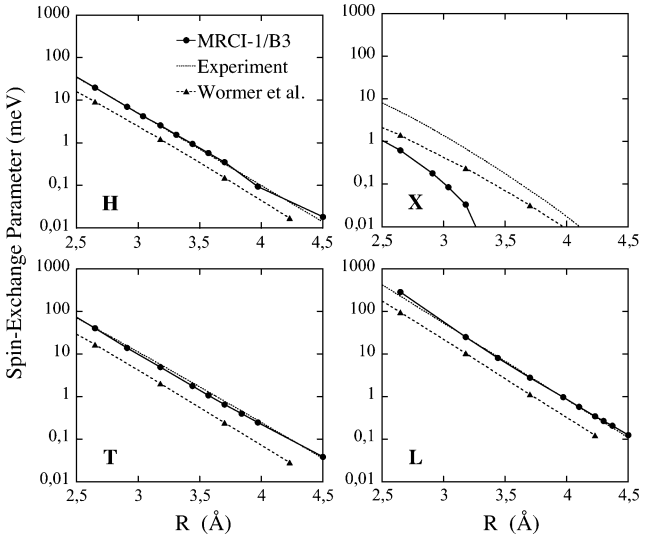

Figure 5. Absolute values of the spin-exchange parameter J obtained from singlet−quintet energy splitting of the MRCI-1/B3 interaction potentials. The results are compared with the experimentally deduced J values[15] and the ab initio calculations of Wormer et al.[13]

between the first singlet, triplet and quintet states of the dimer O_2-O_2 arises from exchange interactions between the two open-shell diatoms which break the multiplet states degeneracy as the diatoms approach each other. According to the pioneering work of van Hemert et al.,[25] the exchange interactions in the dimer O_2-O_2 are known to be well represented by the Heisenberg exchange operator $\hat{H}_{ex} = -2J\boldsymbol{S_a}\cdot\boldsymbol{S_b}$, where $\boldsymbol{S_a}$ and $\boldsymbol{S_b}$ are the electron spin operators of the two diatoms. The Heisenberg Hamiltonian allows to describe the energy splitting between the multiplet states from one unique spin-exchange interaction parameter J:

$$\begin{aligned} V(S=0) &= V + 4J \\ V(S=1) &= V + 2J \\ V(S=2) &= V - 2J \end{aligned} \qquad (1)$$

where V is a spin-average interaction potential, i.e., excluding spin-exchange interactions. In several theoretical studies on the dimer O_2-O_2, the spin-exchange parameter J has been extracted from first-order perturbation theory calculations and the use of eq 1[12,13,25] or by more approximate methods.[26] The experimentally deduced PES[15] also uses eq 1 to represent the energy splitting between the multiplet states. In that case, the J values were adjusted to reproduce the glory amplitudes of the measured integral cross sections as well as the second virial coefficient.

From Eq. 1, it can be anticipated that values of the spin-exchange parameter J could be extracted from the energy differences between the multiplet MRCI potentials, and then combined with the quintet state energies obtained from the CCSD(T) method, to build more reliable interaction potentials for the singlet and triplet states. In this regard, it is important to point out that the exchange interactions are not expected to be as sensitive as the dispersion interactions with respect to high order electron correlation effects. We have thus decided to extract the J parameter from the multiplet MRCI potentials to test the validity of the Heisenberg Hamiltonian as well as to compare with previously obtained J values.

We report in Figure 4 the spin-exchange parameter deduced from the MRCI-1/B3 interaction potentials. To plot them in a logarithmic scale, absolute values of J have been reported. First of all it is worth noticing that, until high values of the interaction energies along the repulsive wall are sampled, very similar J values are obtained from singlet−triplet, triplet−quintet, or singlet−quintet energy splittings. This finding, consistent with earlier theoretical work,[13,25] validates the use of he Heisenberg Hamiltonian to describe the spin exchange interactions in the dimer O_2-O_2. The deviations observed at short R values arise from the presence of a low-lying excited state of triplet symmetry associated with the first excited dissociation limit X $^3\Sigma_g^- +$ a $^1\Delta_g$. Consequently we will keep the J values given by the singlet−quintet energy splitting in what follows. As an additional check, we have obtained J values from MRCI calculations at different levels of theory, for the case of the H orientation, where the dependence of the calculated multiplet energies on the basis set and active space used is most significant (see Figure 2). It was found that the increase of both the basis (B1 to B3) and the active space (MRCI-1 to MRCI-2) produces changes of less than 5% on the J parameter, validating the procedure employed to determine this quantity.

The results obtained from the MRCI-1/B3 potentials are compared in Figure 5 with the experimentally deduced J values and the ab initio calculations of Wormer and van der Avoird.[13] As can be seen, a remarkable agreement with the empirical values has been achieved for the H, T, and L configurations, for which larger couplings are found. Discrepancies of less than 5% with experimental values are found in the potential well regions for the H and L geometries, and around 10% for the T geometry. The sign of the spin-exchange parameter is also correctly reproduced, pointing to an antiferromagnetic coupling ($J < 0$) for the H, T, and L configurations in accordance with experiment. The exception is the X geometry where our theoretical J values are smaller than experiment by about 1 order of magnitude, with $J < 0$ from R_∞ down to 3.4 Å where it then changes sign whereas experiment points to a ferromagnetic coupling ($J > 0$) for all intermolecular separations. With regard to the ab initio calculations of Wormer and van der Avoird,[13] the J values are significantly smaller (around 50% smaller) than those obtained here for all geometries except for the X orientation (where larger values are found). This discrepancy may be due to the shape of the diatom molecular orbitals which were optimized at the Hartree−Fock (HF) level of theory as a

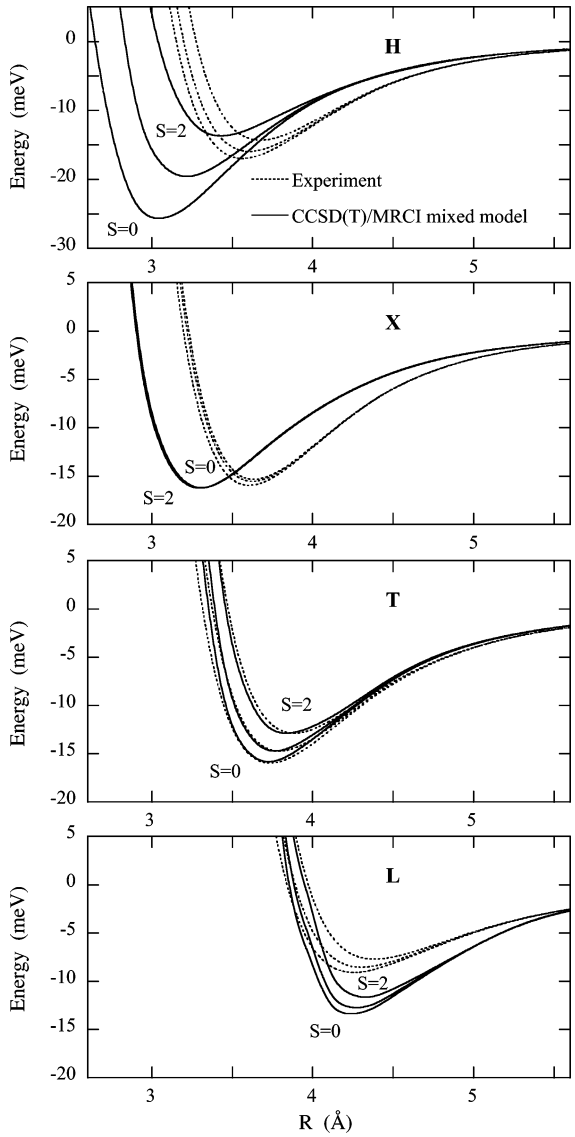

Figure 6. Interaction potentials associated with the first singlet ($S = 0$), triplet ($S = 1$) and quintet ($S = 2$) states of the dimer O_2-O_2 in four selected geometries as obtained from the CCSD(T)/MRCI mixed and the molecular beam experiment.[15]

preliminary step to the first order perturbative calculations. Indeed, the spin-exchange parameter is directly related to the overlap between the molecular orbitals of the diatoms, which explains the nearly exponential R dependence shown in Figure 5. The exception is again the X geometry for which the negligible overlap due to symmetry produces a more complicated R dependence of the J parameter. Also our calculations include electron correlation effects which are completely neglected in the HF calculations of Wormer and van der Avoird.[13]

The values of the spin-exchange parameter J deduced from the MRCI-1/B3 energies were combined with the CCSD(T) energies obtained for the quintet state to determine the singlet and triplet interaction potentials:

$$V_{\mathrm{mix}}(S=0) = V_{(\mathrm{ccsdt})}(S=2) + 6J_{(\mathrm{mrci})}$$
$$V_{\mathrm{mix}}(S=1) = V_{(\mathrm{ccsdt})}(S=2) + 4J_{(\mathrm{mrci})} \qquad (2)$$

Results are shown in Figure 6, and the equilibrium properties associated with each geometry are reported in Table 2. For the

TABLE 2: Equilibrium Distances R_e (in a) and Binding Energies D_e (in meV) for the Singlet, Triplet, and Quintet States of the Dimer O_2-O_2 As Obtained from CCSD(T) Calculations and the CCSD(T)/MRCI Mixed PES (See Text)

		H		X		T		L	
		R_e	D_e	R_e	D_e	R_e	D_e	R_e	D_e
singlet	BW[a]	3.23	19.0	3.33	14.7	4.02	8.0	4.55	5.8
	this work	3.04	25.6	3.31	16.2	3.73	15.8	4.24	13.4
	expt[b]	3.56	17.0	3.63	15.3	3.74	16.0	4.26	9.1
triplet	BW	3.28	17.3	3.33	15.0	4.02	7.9	4.55	5.7
	this work	3.22	19.6	3.31	16.2	3.76	14.7	4.27	12.7
	expt	3.61	15.9	3.62	15.5	3.79	14.7	4.30	8.6
quintet	BW	3.39	14.8	3.28	15.6	4.02	7.6	4.66	5.6
	CCSD(T)[c]	3.43	13.7	3.30	16.2	3.84	12.9	4.33	11.7
	expt	3.68	14.3	3.60	16.0	3.88	12.9	4.38	7.7

[a] Values corresponding to the PES of ref 12. [b] Values corresponding to the PES of ref 15. Absolute uncertainties are estimated as ±0.07 Å on R_e and ±0.8 meV on D_e. [c] Values corresponding to the PES of ref 17.

H geometry, the singlet and triplet states are found to be significantly deeper than experiment and displaced through much smaller R values. Given that our theoretical calculations predict J values in excellent agreement with experiment such a discrepancy is directly related to the difference in R_e between the CCSD(T) and experimental quintet potentials: since the theoretical potential well is located at smaller intermolecular distances and the J parameter grows exponentially with decreasing R's, the splitting due to spin coupling is greatly enhanced for the present potential. In ref 17, we have discussed with some detail the possible reasons for the discrepancy in the R_e value of the quintet potential. An issue that is important to bear in mind is that the functions actually fitted to the experimental data were the radial terms of the spherical harmonics expansion and not the specific geometries we are considering here. In that work,[17] the first four radial terms of the expansion were obtained from the CCSD(T) potentials for the four geometries considered here and compared with the experimental results. It was found that the origin of the different equilibrium distances for the H configuration is the different short-range behavior of the radial terms of the theoretical and the empirical potentials. Similar comments apply for the X geometry where the shape of the theoretical potential agrees with the experimental one although significantly displaced toward smaller equilibrium positions (see Figure 6). For the T geometry an excellent agreement with experiment is found for the three interaction potentials on the binding energies as well as on the equilibrium positions. Finally, the results for the L geometry agree with experiment on the equilibrium bond lengths, and hence on the multiplet energy splitting since J values agree, but the binding energies are found to be significantly larger. This arises from the quintet state energies provided by the CCSD(T) calculations, and again the difference can be traced back to subtle differences in the radial terms.[17]

In Table 2, we have also included the equilibrium properties of the BW surface.[12] Comparison with the present potential indicates a good agreement for the H and X orientations, particularly for R_e, but smaller values of D_e for the singlet and triplet states which can be easily traced back to their smaller J values as discussed above. On the other hand for the T and L configurations the BW surfarce largely underestimates the binding energies.

In this point, it is worthwhile to comment on the spectroscopy experiments of Biennier et al,[16] where a rotationally resolved

spectra for the singlet−singlet transition $[O_2(^1\Delta_g)_{v=0}]_2 \leftarrow [O_2(^3\Sigma_g^-)_{v=0}]_2$ was recorded and partially assigned. The analysis of the spectra, assisted by bound state calculations on the BW potential, led them to confirm that the H geometry is the most stable one for the ground singlet state, in accordance with both the Perugia and the present theoretical potentials. Experimentally obtained rotational constants were found to be larger than those obtained using the BW potential, indicating that the H equilibrium distance should be smaller than the theoretical estimation of 3.23 Å, which is in line with the present findings but contrary to expectations based in the Perugia potential (see Table 2). On the other hand, the experimentally obtained dissociation energy is $D_e = 8.0 \pm 2$ meV,[16] which compares well with the dissociation energy based on the BW potential (9.2 meV) while the Perugia potential leads to a dissociation energy of 14.20 meV[27] (A detailed discussion on the comparison with the spectroscopical work and with the BW potential is given in that work). Clearly, the potential anisotropy plays a crucial role in the determination of bound states so, at this moment, we cannot foresee the value that would be obtained with the present potential, until more orientations are considered to build a singlet potential energy surface and bound state calculations are performed on it.

C. Collisional Cross Sections. To better assess the reliability of the MRCI and CCSD(T)/MRCI mixed potentials previously discussed, we decided to test them on experimental findings such as the total integral cross sections reported in ref 15 for scattering of rotationally hot O_2 effusive beams by O_2 target molecules. The experimental conditions used to measure these data are such that they mainly probe the isotropic component of the interaction; i.e., the colliding system approaches the atom−atom limit. Hence for each of the multiplet states we determined the isotropic radial component $V^{000}(R)$ of the corresponding interaction potential following the first expression of eq 6 in ref 15:

$$V^{000}(R) = \frac{1}{9}[2V_H(R) + 2V_X(R) + 4V_T(R) + V_L(R)] \quad (3)$$

where H, X, T and L refer to the four configurations studied. It is worth noticing that the $V^{000}(R)$ terms so obtained represent an approximation to the spherical interaction components. They would be the exact isotropic contributions if the total anisotropic interaction was expanded in spherical harmonics and only the first four terms were considered, as it was previously done for the experimentally deduced PES.[15]

The $V^{000}(R)$ isotropic terms associated with each of the multiplet states obtained from the MRCI-1/B3 calculations are reported in Figure 7a together with those obtained in the experiment. We observe that the spin-exchange interactions produces in both sets similar effects such as binding energies larger for the singlet states than for the quintet ones, thus pointing to an antiferromagnetic spin coupling character of the isotropic interaction. Nevertheless, rather deeper wells and more attractive profiles in the long range part of the potentials can be globally noticed for the experimentally deduced PES's. To take into account the spin-exchange interactions in the analysis of the experimental scattering data, it must be noted that, as a consequence of the conservation of total spin quantum number S of the system during a collision, transitions between surfaces with different spin values are not allowed. Hence the measured total cross sections $Q(v)$ as a function of the collision velocities v are the weighted sum of the three partial cross sections

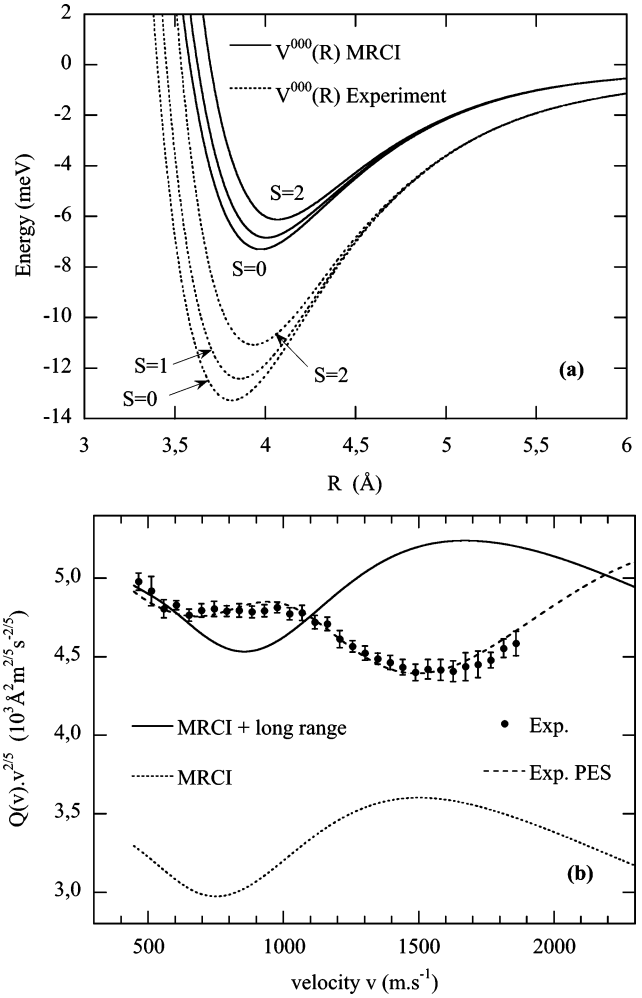

Figure 7. Comparison of the multiplet isotropic terms $V^{000}(R)$ obtained from the MRCI-1/B3 calculations and experiment[15] (upper panel); Comparison of the total integral cross sections measured from the rotationally hot molecular beam experiment and obtained from semiclassical calculations using the experimentally deduced PES and the MRCI-1/B3 PES (lower panel).

$Q^{S=0}(v)$, $Q^{S=1}(v)$, and $Q^{S=2}(v)$ associated with the singlet, triplet, and quintet states respectively:

$$Q(v) = \frac{Q^{S=0}(v) + 3Q^{S=1}(v) + 5Q^{S=2}(v)}{9} \quad (4)$$

where the weighting factors are given by the multiplet spin degeneracies. We report in Figure 7b the experimental total integral cross sections measured for a wide range of collision velocities, corresponding to collision energies ranging approximately from 20 to 300 meV. The multiplet isotropic terms $V^{000}(R)$ associated with both the MRCI and experimentally deduced PES's have been employed in semiclassical calculations following a JWKB method to compute the corresponding total cross sections shown in Figure 7b. It is worth pointing out that, in the atom−atom collision regime assumed for the experimental scattering data, the glory structure of the cross sections provide infomation on the potential well features[28,29] while their absolute values contain information about the long-range attraction.[30] Moreover, the quenching of the glory amplitudes at low collision velocities are known to be related with the isotropic component of the spin-exchange interaction. As can be seen in Figure 7b, the comparison between the experimental cross sections and those obtained from the MRCI potentials suggests an underes-

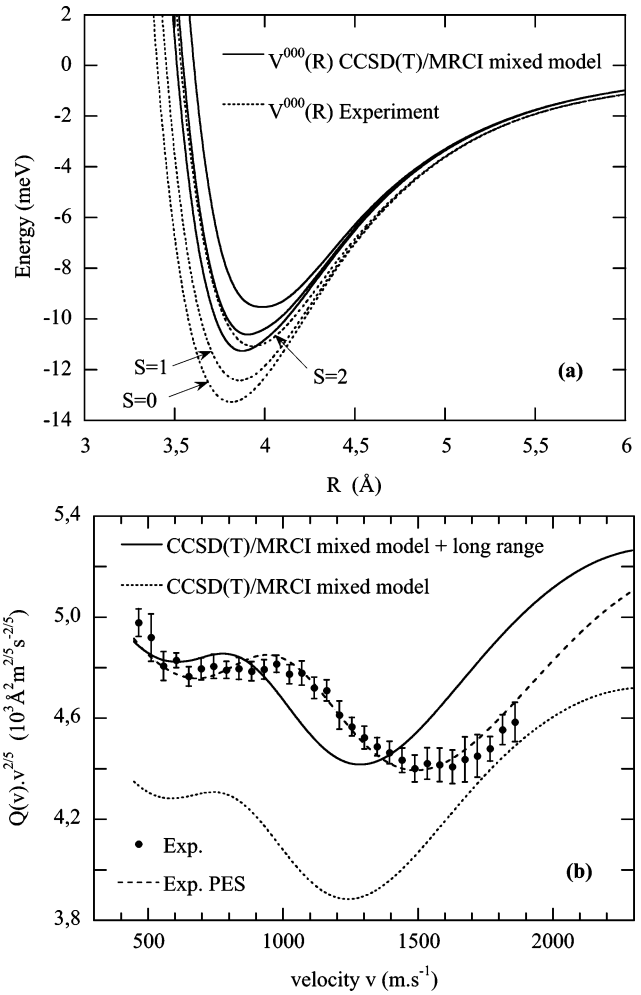

Figure 8. Comparison of the multiplet isotropic terms $V^{000}(R)$ obtained from the CCSD(T)/MRCI mixed potentials and experiment[15] (upper panel). Comparison of the total integral cross sections measured from the rotationally hot molecular beam experiment and obtained from semiclassical calculations using the experimentally deduced PES and the CCSD(T)/MRCI mixed PES (lower panel).

timation of both theoretical long-range attraction and well area. Properly adjusting the long-range part of the MRCI potentials with an analytical form as $-C_6/R$,[6] and then using a 64% higher C_6 dispersion coefficient, it is possible to obtain a good agreement with the absolute values of the experimental cross sections. Nevertheless, the predicted glory pattern of the cross section still exhibits a dephased behavior with respect to the experimental one. This marked difference suggests that the potential well area of the different MRCI multiplet isotropic terms $V^{000}(R)$ needs to be much larger.

A similar analysis has been performed for the CCSD(T)/MRCI mixed PES, and the results obtained for the multiplet isotropic $V^{000}(R)$ terms are shown in Figure 8a. It is readily seen to give a better agreement with the experimentally deduced $V^{000}(R)$ terms than that obtained from the MRCI potentials. The theoretical potential wells are now more shallow than experiment by only a small amount (less than 2 meV) while the equilibrium bond lengths are found larger by 0.05 Å. The better agreement in the description of long-range interactions is noticeable with differences of about 1 cm^{-1} for $R > 6$ Å. This considerable improvement with respect to the MRCI potentials is reflected in the associated total cross sections shown in Figure 8b. As can be seen, the absolute values of the cross sections calculated from the CCSD(T)/MRCI mixed potentials are much closer to experiment. A further improvement is obtained by adjusting the long-range part of the potentials to a $-C_6/R^6$ analytical form where the C_6 dispersion coefficient is increased by 26%. From this corrected potential, we can appreciate only a slight shift with respect to experiment in the glory structure of the cross sections at lower collision velocities. It has to be noticed that an optimal description of the glory pattern (location of the extrema) would be obtained in the case where the potential wells area associated with the present isotropic $V^{000}(R)$ terms would be 13% larger. From the present analysis, it follows that the largest inaccuracy in the CCSD(T)/MRCI mixed PES corresponds to its description of long-range interactions since it leads to cross section absolute values understimated by about 10% at low to moderate collision energies. Nevertheless, it is clear that a further improvement of long-range interactions, which actually differ by about 1 cm^{-1} with experiment, would be very difficult from theoretical ab initio methods.

IV. Summary and Conclusions

An accurate set of intermolecular potentials for the singlet and triplet states of the O_2-O_2 dimer have been obtained on the basis of strictly ab initio information. Advantage was taken of the fact that the Heisenberg Hamiltonian provides an accurate representation of the exchange interactions allowing the combination of CCSD(T) and MRCI ab initio information to construct the potentials. The potentials developed have been tested by computing total integral cross sections and comparing them with the detailed experimental study of the Perugia group.[15] Comparison with experiment is very good, especially when one considers the subtle dependence of glory oscillations and absolute values of the cross sections on the details of the intermolecular potential. On the other hand, comparison with the experimentally derived intermolecular potentials is less straightforward. For some angular orientations (most notably the T-shaped), agreement is excellent, but for other orientations, there are significant discrepancies either in the equilibrium geometries (H and X) or in the binding energies (most notably the linear geometry).

To analyze these differences, we use the same spherical harmonic expansion of the potential used in the experiment.[15] Concerning the interaction in the well region, the theoretical isotropic terms ($V^{000}(R)$) slightly underestimate the average van der Waals interaction probed by the rotationally hot molecular beam experiment: the present analysis suggest that a larger long range attraction (as the one used for the cross section absolute value fit) combined with a slightly lighter short range repulsion would improve the description of the averaged van der Waals interaction. On the other hand, it is important to point out that these radial terms have been obtained using a four term spherical harmonic expansion and a limited set of angular orientations (4), which could also be partly responsible for the observed discrepancies specially when these have been shown to be very small.

Regarding the reliability of the theoretical anisotropic components it would be important to test its capacity in predicting both integral cross sections measured with rotationally cold aligned molecular beams[15] and second virial coefficients at low temperatures.[31] For this, an analytical representation of the theoretical PES is needed. An analytical extrapolation, following the procedures described in ref 15, could be attempted. This should prove of crucial importance since subtle differences in the anisotropic components are responsible of the main discrepancies observed for the H, X, and L orientations.[17] Finally, it would be important to perform sensitivity analysis of the potential parameters in the simulation of the experimental

observables as well as more detailed analysis of the different components of the interaction energy such as exchange−repulsion and dispersion which dominate the shape of the potentials.

Acknowledgment. The authors wish to acknowledge financial support by CONACYT (Mexico, Grant 44117E), SESIC-SEP-FOMES2000 for unlimited time on the IBM p690 supercomputer at UAEM, the Ministerio de Educación y Ciencia (Spain, Grant CTQ-2004-02415/BQU), CESGA for computing time, and MIUR (Italy). R.H.L. wishes to thank Maciej Gutowski for many valuable comments regarding intermolecular forces.

References and Notes

(1) The whole issue: *Chem. Rev.* **2000**, *100* (11).
(2) Chalasinski, G.; Szczesniak, M. M. *Chem. Rev.* **2000**, *100*, 4227.
(3) Watts, J. D.; Gauss, J.; Bartlett, R. J. *J. Chem. Phys.* 98, **1993**, 8718 .
(4) Jeziorski, B.; Moszynski, R.; Szalewicz, K. *Chem. Rev. 94*, **1994**, 1887.
(5) Lewis, G. N. *J. Am. Chem. Soc*. **1924**, *46*, 2027.
(6) Pauling, L. *The nature of the chemical bond*; Cornell University Press: Ithaca, NY, 1960.
(7) Long, C. A.; Ewing, G. E. *J. Chem. Phys.* **1973**, *58*, 4824.
(8) Goodman, J.; Brus, L. E. *J. Chem. Phys.* **1977**, *67*, 4398.
(9) Slanger, T. G.; Copeland, R. A. *Chem. Rev.* **2003**, *103*, 4731.
(10) Antonov, I. O.; Azyazov, V. N.; Ufmtsev, N. I. *J. Chem. Phys.* **2003**, *119*, 10638.
(11) Gorelli, F. A.; Ulivi, L.; Santoro, M.; Bini, R. *Phys. Rev. Lett.* **1999**, *83*, 4093.
(12) Bussery, B.; Wormer, P. E. S. *J. Chem. Phys.* **1993**, *99*, 1230.
(13) Wormer, P. E. S.; van der Avoird, A. *J. Chem. Phys.* **1984**, *81*, 1929.
(14) Cambi, R.; Cappelletti, D.; Liuti, G.; Pirani, F. *J. Chem. Phys.* **1991**, *95*, 1852.
(15) Aquilanti, V.; Ascenzi, D.; Bartolomei, M.; Cappelletti, D.; Cavalli, S.; de Castro Vitores, M.; Pirani, F. *J. Am. Chem. Soc.* **1999**, *121*, 10794.
(16) Biennier, L.; Romanini, D.; Kachanov, A.; Campargue, A.; Bussery-Honvault, Bacis, B. R. *J. Chem. Phys.* **2000**, *112*, 6309.
(17) Hernández-Lamoneda, R.; Hernández, M. I.; Campos-Martínez, *J. Chem. Phys. Lett*. **2005**, *414*, 11.
(18) Widmark, P. O.; Malmqvist, P. A.; Roos, B. O. *Theor. Chim. Acta* **1990**, *77*, 291.
(19) Chalasinski, G.; Szczesniak, M. M. *Chem. Rev.* **1994**, *94*, 1723.
(20) Tao, F. M.; Pan, Y. K. *J. Chem. Phys.* **1992**, *97*, 4989.
(21) Langhoff, S. R.; Davidson, E. R. *Int. J. Quantum Chem.* **1974**, *8*, 61.
(22) Davidson, E. R.; Silver, D. W. *Chem. Phys. Lett.* **1977**, *52*, 403.
(23) Boys, S. F.; Bernardi, F. *Mol. Phys.* **1970**, *19*, 553.
(24) van Lenthe, J. H.; van Duijneveldt-van de Rijdt, J. G. C. M.; van Duijneveldt, F. B. *Adv. Chem. Phys.* **1987**, *69*, 521.
(25) van Hemert, M. C.; Wormer, P. E. S.; van der Avoird, A. *Phys. Rev. Lett.* **1983**, *51*, 1167.
(26) Bussery, B.; Umanskii, Ya, S.; Aubert-Frécon, M.; Bouty, O. *J. Chem. Phys.* **1994**, *101*, 416.
(27) Aquilanti, V.; Carmona-Novillo, E.; Pirani, F. *Phys. Chem. Chem. Phys.* **2002**, *4*, 4970.
(28) Bernstein, R. B.; O'Brien, T. J. P. *Discuss. Faraday Soc.* **1965**, *40*, 35.
(29) Bernstein, R. B.; O'Brien, T. J. P. *J. Chem. Phys.* **1967**, *46*, 1208.
(30) Pirani, F.; Vecchiocattivi, F. *Mol. Phys.* **1982**, *45*, 1003.
(31) Dymond, J. H.; Smith, E. B. *The Virial Coefficient of Pure Gases and Mixtures: a Critical Compilation*; Clarendon Press: Oxford, U.K., 1980.